Microwave Breakdown in Resonators and Filters

D. Anderson, U. Jordan, M. Lisak, T. Olsson, *Associate Member, IEEE,* and M. Åhlander

***Abstract*— Several aspects of microwave breakdown in resonators are discussed in this paper. Approximate analytical criteria are formulated for the critical microwave breakdown field in some illustrative model geometries, which clearly brings out the main physical properties of microwave-induced breakdown in the presence of inhomogeneous electric fields. The analytical results are verified by comparisons with numerical calculations. A full numerical solution procedure for determining the microwave breakdown field in commercially available resonator designs is also presented. The numerical predictions are compared with experimental results, demonstrating very good agreement in the pressure range available for the experiments. The success of the predictions of the breakdown threshold suggests methods complementary to high-power pulse testing of radio-frequency filters.**

***Index Terms*— Microwave breakdown, microwave filters, microwave resonators.**

I. Introduction

MICROWAVE breakdown in gases under various physical and technical conditions is a well-known and much-studied problem. A classical summary of relevant results is given in [1]. However, the technical development of microwave generators as well as of microwave devices continue to give rise to new situations and parameter regimes where microwave breakdown plays an important role and where previous results on breakdown are not directly applicable.

One example of this is the recent development of microwave pulse generators, which are now capable of delivering very short and very intensive pulses for which classical breakdown theory has to be properly generalized [2]. Another example is provided by the trend to design microwave devices as small and compact (and low cost) as possible. This development leads to concern about the concomitant breakdown strength of the construction, in particular, in situations involving more complicated geometries, such as in microwave resonators and filters.

In many microwave devices, the geometrical configuration gives rise to local strongly enhanced microwave fields. Such regions are potentially dangerous from the point-of-view of breakdown since the field here may be much stronger than the globally predicted breakdown field. On the other hand, a locally overcritical field does not necessarily imply global breakdown. Several model examples of this situation are considered and the influence of local field enhancement on the global breakdown condition is investigated. In this paper, we will discuss several aspects of microwave breakdown with emphasis on the problem of breakdown in the inhomogeneous microwave fields determined by a resonator or filter geometry.

First, we will consider microwave breakdown in a cylindrical resonator where the inhomogeneous electric field gives rise to a strongly inhomogeneous ionization. We analyze this problem using an approximate analytical variational approach, which has the advantage of giving very simple and explicit expressions for the predicted breakdown electric fields and also gives a clear picture of the physics involved in the breakdown process. For more complicated geometries, the usefulness of analytical approximations become limited and resort must be taken to numerical means. We illustrate this by a direct numerical determination of the breakdown field in a realistic microwave resonator. The numerical predictions are related to the analytical understanding obtained and are also compared with experimental results. Very good agreement between theory and experiments is demonstrated.

Finally, we use the obtained results to suggest a procedure for predicting and testing microwave breakdown in resonators used, e.g., in antenna feed systems for mobile telephone communication. These resonators conventionally operate at or near atmospheric pressures and a realistic test of their critical breakdown strength is sometimes expensive and cumbersome to perform due to the high powers needed. On the other hand, the breakdown threshold decreases with decreasing pressure, thus making it easier to perform a breakdown test at lower pressures. We have shown that by performing breakdown measurements at low powers, a reliable extrapolation of these results to atmospheric pressures can be made based on the numerically obtained curve for the breakdown strength as a function of gas pressure. The analytical considerations show that breakdown due to diffusion at lower pressures can be characterized by an effective diffusion length, which, however, depends on the complicated geometry and, in practice, can only be determined numerically. As the pressure is increased, breakdown becomes controlled by a combination of diffusion and attachment losses, the relative ratio between these factors being determined by the numerically obtained result. We hope that this method proves a useful tool for easy tests of the breakdown strength of various gas-filled microwave devices working at atmospheric pressures.

Manuscript received March 26, 1999; revised July 16, 1999.

D. Anderson, U. Jordan, and M. Lisak are with the Department of Electromagnetics, Chalmers University of Technology, S 412 96 Göteborg, Sweden.

T. Olsson and M. Åhlander are with the Allgon System AB, 18325 Täby, Stockholm, Sweden.

Publisher Item Identifier S 0018-9480(99)08454-9.

II. Basic Breakdown Physics

Gas breakdown in microwave electric fields manifests itself as an avalanche-like increase in time of the free electron density. This increase is caused by collision ionization of the neutral gas molecules by free electrons that are being

0018–9480/99$10.00 © 1999 IEEE

accelerated to high energies by the microwave field. The evolution of the free electron density $n(x, t)$ is governed by the continuity equation [1]

$$\frac{\partial n}{\partial t} = \nabla \cdot (D\nabla n) + \nu_i n - \nu_a n \tag{1}$$

where D is the diffusion coefficient, ν_i is the ionization frequency, and ν_a is the attachment frequency of the free electrons on neutral molecules.

A heuristic way of deriving the breakdown threshold condition is to introduce the effective density scale length L_{eff} as

$$\nabla \cdot (\nabla n) \equiv -\frac{1}{L_{\text{eff}}^2}\, n. \tag{2}$$

This simplified analysis makes it possible to rewrite (1) as

$$\frac{\partial n}{\partial t} = \nu_{\text{net}} n \tag{3}$$

where

$$\nu_{\text{net}} = \nu_i - \nu_D - \nu_a \tag{4}$$

and $\nu_D = D/L_{\text{eff}}^2$ is an effective diffusion frequency corresponding to the density scale length L_{eff}. From (3), we infer that the electron density will grow exponentially when $\nu_{\text{net}} > 0$, which defines the breakdown threshold as

$$\nu_{\text{net}} = 0. \tag{5}$$

The weak point in this approach is that there is no easy way to predict the crucial parameter L_{eff}, which determines the density scale length and the concomitant diffusion losses. Qualitatively, we expect L_{eff} to be determined by the shortest diffusion distance in the system, i.e., essentially by half the geometrical dimension of the waveguide, resonator, etc.

However, such crude estimates are generally not enough in order to determine L_{eff} and an accurate determination involves solving the eigenvalue problem obtained from (1) in the limit case when $\partial n/\partial t = 0$, which reads

$$\nabla^2 n + \frac{\nu_i - \nu_a}{D}\, n = 0$$

and

$$n(\partial V) = 0 \tag{6}$$

where ∂V denotes the boundary of the region V occupied by the microwave electric field. Obviously, with $(\nu_i - \nu_a)/D = \lambda$, (6) becomes a classical eigenvalue problem. From the solution, we can now define L_{eff} rigorously from (6) as

$$L_{\text{eff}}^{-2} \equiv -\frac{\nabla^2 n}{n} = \lambda. \tag{7}$$

We emphasize the fact that, in this case, the effective density scale length L_{eff} is determined by the geometry of the configuration only.

A further complication of the problem of determining accurate breakdown thresholds is due to the fact that although the diffusion coefficient and attachment frequency depend rather weakly on the strength of the microwave electric field E and, consequently, can be considered as constants, the ionization frequency increases rapidly for increasing electric-field strength. A commonly used approximation for the ionization frequency is

$$\nu_i = \nu_i(E) \approx \nu_{i0} \left(\frac{E}{E_0} \right)^{\beta} \tag{8}$$

where E_0 is a normalizing electric field and ν_{i0} is the ionization frequency corresponding to that field. The parameter β depends on the gas, but typically for air $\beta = 5.33$.

Since the electric field has an inhomogeneous mode structure determined separately by the electrodynamic (undisturbed) equations for the microwave field, the ionization frequency appearing in (1) is, in realistic situations, inhomogeneous, i.e., $\nu_i = \nu_i(x)$. Although this generalization complicates the detailed analysis of the breakdown problem, it does not imply a conceptually different situation as compared to the homogeneous case. The full diffusion equation can now be written

$$\frac{\partial n}{\partial t} = \nabla \cdot (D\nabla n) + (\nu_i(x) - \nu_a) n. \tag{9}$$

Generalizing our previous heuristic approach, we can again introduce an effective density scale length and approximate (9) as

$$\frac{\partial n}{\partial t} \approx -\frac{Dn}{L_{\text{eff}}^2} + (\max \nu_i - \nu_a) n \tag{10}$$

where $\max \nu_i$ denotes the maximum of the ionization frequency over the volume occupied by the microwave field. The breakdown threshold condition clearly becomes

$$\nu_{\text{net}} \equiv \max \nu_i - \nu_D - \nu_a = 0 \tag{11}$$

where ν_D is still defined by (2).

The characteristic scale length L_{eff} is now even more difficult to determine accurately than in the homogeneous case since it depends on the spatial mode structure of the electric field (which is given) in addition to the dependence on the spatial mode structure of the electron density. The rigorous analysis for determining the breakdown threshold involves solving the following new eigenvalue problem:

$$\nabla^2 n + \lambda s(x) n = 0$$

and

$$n(\partial V) = 0 \tag{12}$$

where $\lambda = [\max \nu_i(x) - \nu_a]/D$, $s(x) = (\nu_i(x) - \nu_a)/[\max \nu_i(x) - \nu_a]$. It is obvious from (12) that the eigenvalue will now also be affected by the field inhomogeneity through the normalization form factor $s(x)$ and that the density scale length depends on x in contrast to the simpler case investigated earlier.

Nevertheless, having found the eigenvalue λ by solving (12), the breakdown condition (11) can be used *a posteriori* to infer the proper effective scale length through the relation

$$L_{\text{eff}}^{-2} \equiv -\frac{\nabla^2 n(0)}{n(0)} = \lambda = \frac{\max \nu_i - \nu_a}{D} \tag{13}$$

where, for simplicity, we have assumed that $\max \nu_i = \nu_i(0)$. Obviously, (13) is equivalent to the heuristic breakdown condition, which includes a diffusion frequency determined by the effective scale length L_{eff}.

However, the inhomogeneous eigenvalue problem given by (12) is difficult to solve analytically for geometries of practical interest and a resort must then be taken to either approximate analytical techniques or to numerical means. In this study, we will demonstrate both possibilities although, admittedly, in complicated geometries, a numerical approach is the only possible way to determine the breakdown threshold. However, we will also show that the concept of an effective scale length, which determines the diffusion losses, can be used in a semianalytical way in combination with experiments to make accurate predictions for the breakdown threshold over a large range of pressures. The basic idea here is to determine the characteristic length L_{eff} by low-pressure breakdown experiments and then to extrapolate the analytical breakdown expression to higher pressures using the experimentally determined scale length.

III. Approximate Analysis Based on Direct Variational Methods

A convenient approach for approximate analysis of the eigenvalue problem (12) is direct variational methods based on trial functions and subsequent Raleigh–Ritz optimization. This approach has been used successfully (both analytically and numerically) in previous studies of breakdown problems. Epstein, who applied the approach to several simple cases where alternative exact solutions were available, made one of the first applications to situations involving spatially varying fields [3]. Approximate, but explicit analytical solutions were obtained and shown to be in very good agreement with the exact solutions. He also demonstrated semianalytical examples where the first step of the analysis could be performed analytically, but where the second optimization step, although conceptually simple, became algebraically tedious and was most conveniently performed numerically. The approach was later used (and generalized) by Mayhan and Fante, [4], [5] in applications to breakdown in narrow infinite [4] and rectangular [5] slot radiators, also including situations involving microwave pulses where the finite pulse length affects the breakdown condition. An example of a purely numerical analysis based on the variational formulation is given by Maldonado and Ayala [6], who investigated diffusion controlled breakdown of gases in cylindrical microwave cavities excited in different TM_{0n0} modes.

The variational analysis is based on the fact that the characteristic eigenvalue problem can be reformulated as a variational problem according to

$$\delta \int_V L\, dV = 0 \tag{14}$$

where the Lagrangian L is given by

$$L = (\nabla n)^2 - \lambda s(x) n^2. \tag{15}$$

Approximate solutions of the eigenvalue problem can now be found by means of Raleigh–Ritz optimization. This implies that the expected solution for $n(x)$ is expressed in terms of a flexible and physically reasonable trial function $n_T(x; p_1, p_2, \cdots)$ with a prescribed dependence on x, but involving one or several unknown parameters p_j, $j = 1, 2, \cdots$. The trial function is inserted into the variational integral, which can then be integrated over x to give the reduced Lagrangian $\langle L \rangle$ according to

$$\langle L \rangle \equiv \int_V L\Big(n(x) = n_T(x; p_1, p_2, \cdots)\, dx\Big). \tag{16}$$

Obviously, $\langle L \rangle$ is an algebraic function of the parameters p_j only and the variational equations now reduce to the algebraic equations

$$\frac{\partial \langle L \rangle}{\partial p_j} = 0, \qquad j = 1, 2, \cdots \tag{17}$$

which, together with the trivial relation $\langle L \rangle = 0$, determine the constants p_j and, more importantly, the eigenvalue λ.

The integration and subsequent optimization may, in principle, be done analytically, semianalytically, or numerically. However, it is obvious that a completely analytical analysis requires a careful choice of trial functions and a not too complicated geometry, whereas a semianalytical or completely numerical analysis makes it possible to investigate more complicated problems. In this study, we will give an illustrative demonstration of the usefulness of the variational approach and the implications for determining the effective scale length of the problem.

IV. Variational Approach to Breakdown in Cylindrical Waveguides and Cavities

As an illustration of the variational approach, we will consider breakdown in a hollow cylindrical waveguide of radius R and height L for a microwave field excited in the TM_{o1o} mode, where the electric field can be written as $E = E_0 J_0(j_0 r/R)$. The eigenvalue problem for the electron density n can be solved by first separating $n(x)$ according to $n(x) = N(r)Z(z)$, where the lowest order mode structure in the axial direction is simply $Z(z) = \cos(\pi z/L)$. This implies that the remaining eigenvalue problem for the radial mode dependence $N(r)$ of $n(x)$ becomes

$$\frac{1}{r}\frac{d}{dr}\left(r\frac{dN}{dr}\right) + \Big[\lambda s(r) - q\Big]N = 0$$

and

$$\frac{dN}{dr}(0) = 0 = N(1) \tag{18}$$

where, for convenience, in this case, we have chosen the normalization $\lambda = R^2 \max \nu_i(x)/D$, $s(x) = \nu_i(x)/\max \nu_i(x) = J_0^{\beta}(j_0 r)$, and, in this case, $q = R^2(\nu_a - \nu_{D\|})/D$. For simplicity, we have normalized the radius to R, and $\nu_{D\|} = D\pi^2/L^2$ denotes the loss frequency due to diffusion in the axial direction.

The eigenvalue problem given by (18) does not have an analytical solution (as far as we know), but has been analyzed earlier by McDonald [1] (for $\nu_a = 0$) by means of a series of approximations, which finally leads to a complicated transcendental equation for determining the eigenvalue, i.e., the breakdown threshold. Here, we will use the direct variational approach to find a simple analytical approximation for the breakdown threshold.

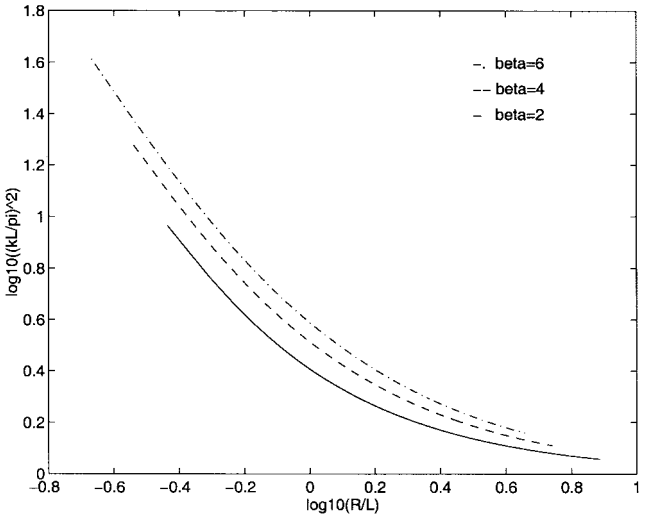

Fig. 1. Plots of the analytical breakdown condition given by (21) for some different values of β. For easy comparison, the notation of [1] is used and $k^2 = \lambda$.

Using the fact that a good approximation for the Bessel function $J_0(j_0 r)$ is

$$J_0(j_0 r) \approx (1-r^2)^m, \qquad m = \left(1+\sqrt{2}\right)/2 \approx 1.21 \quad (19)$$

it becomes obvious that a natural trial function to use in the present case is $N(r) = (1-r^2)^\alpha$ where the parameter to be optimized is α. The reduced Lagrangian becomes

$$\langle L \rangle = \frac{1}{2}\left[\frac{2\alpha}{2\alpha-1} - \frac{\lambda}{m\beta+2\alpha+1} + \frac{q}{2\alpha+1}\right]. \quad (20)$$

The two conditions $\langle L \rangle = 0 = \partial\langle L \rangle/\partial\alpha$ give two algebraic equations that can be manipulated into the form

$$\lambda = \left[1 - \frac{2}{(2\alpha-1)^2}\right]\frac{(m\beta+2\alpha+1)^2}{m\beta}$$
$$q = \frac{(2\alpha+1)^2}{(2\alpha-1)^2}\,\frac{4\alpha^2-4\alpha-1-m\beta}{m\beta}. \quad (21)$$

Equation (21) can be interpreted as a parametric representation for the eigenvalue $\lambda = \lambda(q, m, \beta)$, which directly determines the breakdown threshold. This relation is shown in Fig. 1. The agreement is very good with the corresponding approximate result obtained in [1]. [Note though that the y-axis in [1, Fig. 6-2] should be $(KL/\pi)^2$ instead of $(\pi/KL)^2$.]

The threshold relation becomes particularly simple in the limit case when the axial diffusion losses are small ($\nu_\parallel = 0$) and attachment losses can be neglected ($\nu_a = 0$). Equation (21) then reduces to the following simple expressions:

$$\alpha = \frac{1+\sqrt{2+m\beta}}{2} \quad (22)$$

and

$$\lambda = \left(1+\sqrt{2+m\beta}\right)^2. \quad (23)$$

In particular, we note that for $m = 0$, the eigenvalue equation reduces to a homogeneous equation, which is the same as the one determining the radial mode structure of the microwave field. The exact lowest order mode of this equation is $J_0(j_0 r)$ and, thus, the variational approach (as a by product) gives a simple approximation of the lowest order Bessel mode according to

$$J_0(j_0 r) \approx (1-r^2)^\alpha \quad (24)$$

where $\alpha = \left(1+\sqrt{2}\right)/2 \approx 1.21$. The corresponding eigenvalue is $\lambda \approx 4\alpha^2 = \left(1+\sqrt{2}\right)^2 \approx 5.83$ to be compared with the exact eigenvalue $\lambda = j_0^2 = 5.78$. The overall agreement between the variational predictions and the numerical results is generally good (cf. Table I). The approximate mode structure begins to deviate from the numerically obtained one, for large values of β, but the approximations for the corresponding eigenvalues still show good agreement, which is typical of the direct variational approach.

TABLE I
COMPARISON BETWEEN EIGENVALUES OF (18) FOR DIFFERENT VALUES OF β AND FOR $L = \infty$. ANALYTICAL EIGENVALUES λ_a AND NUMERICAL ONES λ_n

β	λ_a	λ_n	Relative error %
0	5.77	5.83	0.9
1	7.85	8.01	2.0
2	9.74	10.0	3.0
3	11.5	12.0	4.0
4	13.2	13.8	5.0
5	14.8	15.7	5.9
6	16.3	17.5	6.9

The approximate breakdown threshold can be written as

$$\frac{R^2\nu_i(0)}{D} = \lambda = \left(1+\sqrt{m\beta+2)}\right)^2. \quad (25)$$

This implies that the effective density scale length L_{eff} becomes

$$L_{\text{eff}} \equiv \sqrt{\frac{D}{\nu_i(0)}} = \frac{R}{\sqrt{\lambda}} = \frac{R}{1+\sqrt{m\beta+2}}. \quad (26)$$

As expected, the effective density scale length depends on the geometrical size of the waveguide (R), but also on the inhomogeneous mode structure of the microwave field (m) and on the degree of nonlinearity in the ionization frequency (β).

V. BREAKDOWN IN LOCALLY ENHANCED MICROWAVE FIELDS

In many microwave devices, the geometrical configuration gives rise to localized strongly enhanced microwave fields. Such regions are potentially dangerous from the point-of-view of breakdown since the field here may be much stronger than the globally predicted breakdown field. On the other hand, a locally overcritical field does not necessarily imply "global" breakdown, i.e., an increase of electron density in time everywhere in the configuration.

However, even below the breakdown threshold, there may exist regions in the volume where the electron density is high.

In fact, if it is high enough to make the concomitant plasma frequency ω_p equal to the microwave frequency ω; important effects on the microwave propagation can be expected, even though the microwave field strength is formally below the breakdown threshold. In a resonator or filter, the high field region is usually confined to a small, but very important, region from the point-of-view of device performance. If, in this region, a high electron density is reached, this may be enough to degrade the performance even though the electron density over the main volume of the resonator is (and remains) small. Another dangerous scenario is the one where a locally high field (and concomitant high electron density) gives rise to significant absorption and the formation of "hot spots" where the temperature of the gas is increased. At high gas temperatures, the gas becomes even more liable to breakdown and the breakdown strength of the gas decreases, ultimately leading to "global" breakdown. Thus, regions of strong electric-field enhancement tend to give rise to regions of high electron density and are potentially dangerous from the point-of-view of microwave breakdown, and should be avoided in a careful design.

In view of the analysis of the preceding sections, it is instructive to discuss the scale length of the density variation in situations with strong local electric-field enhancement. It is physically clear that even if the electrons are created in the high field region, diffusion is liable to spread the electrons out into the low field region where they are absorbed by attachment and/or diffusion to the walls. The corresponding scale length will then depend on the length of the enhanced electric-field region and the diffusion distance to the wall as well as on the relative strength of the diffusion and attachment processes.

In fact, it can easily be shown by analyzing some simple model geometries that, in situations where the ionization is restricted to a small region of extension a and the losses are dominated by diffusion to a wall a distance L away from the electron-producing high-field region, the density scale length is simply the geometric mean of the two characteristic distances. This implies the breakdown condition

$$\sqrt{\frac{D}{\nu_i}} \equiv L_{\text{eff}} = \sqrt{aL} = a\sqrt{\frac{L}{a}} \gg a \tag{27}$$

where ν_i is the ionization frequency in the high-field region. A similar result, in the quite different situation of breakdown in free space, was obtained in [9]. Note again that the characteristic scale length is determined by the geometry of the configuration only (cf. the result of the analysis of Section IV).

Consider now the situation where losses from the high-field region take place by means of diffusion into a low-field region where attachment is the dominating loss mechanism. We can then show, in a similar way, that the breakdown condition and density scale length are determined by

$$\sqrt{\frac{D}{\nu_i}} \equiv L_{\text{eff}} = \sqrt{aL_a} = a\sqrt{\frac{L_a}{a}} \gg a \tag{28}$$

i.e., as the geometric mean of the length of the high-field region and a characteristic attachment length L_a determined by

$$L_a = \sqrt{D/\nu_a}. \tag{29}$$

Finally, we note that L_{eff} qualitatively determines the extension of a high-density region or hot spot. In the case when the electron losses from the field enhancement region is due to diffusion only, geometric lengths determine the scale length. On the other hand, in the case when the field enhancement region is drained by electrons through diffusion into an attachment dominated region, the characteristic extension of the high electron density region is given by $L_{\text{eff}} = \sqrt{aL_a}$, where L_a is determined by (29). Furthermore, both D and ν_a depend on the gas pressure p ($D \propto 1/p$ and $\nu_a \propto p$), which implies that $L_{\text{eff}} \propto 1/p$. Consequently, in this situation, we expect the extension of the hot spot around a region of local electric-field enhancement to increase with decreasing gas pressure. Both these characteristic properties will be demonstrated further in the full numerical and experimental investigations.

VI. Numerical Approach to The Breakdown Problem in Circular–Symmetric Resonators

A. Introduction

Until now, we have only been considering analytical and semianalytical results and their numerical verifications for breakdown in some simple geometries. Much of the characteristic physics involved in the breakdown process has been clarified and highlighted and several important explicit results have been derived. Nevertheless, for accurate predictions in more realistic practical situations, it is important to have access to numerical programs, which are capable of handling more general and complicated geometries. For this purpose, we have implemented a numerical tool for solving two-dimensional cylindrical–symmetric problems. The numerical procedure consists of two parts. In the first part, the electric-field distribution for the lowest order TM mode in a cylindrical–symmetric resonator is computed and, in the second part, the obtained electric field structure is used to solve the eigenvalue problem determining the breakdown threshold in the same resonator.

B. Numerical Approach for the Determination of the Lowest Order TM Mode in a Circular–Symmetric Resonator

The present numerical procedure is primarily intended for a circular–symmetric resonator filled with a homogeneous dielectric material (in our case air) without free charges. Since we are only interested in the lowest order TM mode, we can assume that $E_\varphi = H_r = H_z = 0$ and that all components of the electric and magnetic fields are independent of φ. From Maxwell's equations, one can then derive the following equation for H_φ [12]:

$$\nabla^2 H_\varphi - \frac{1}{r^2} H_\varphi + \omega^2 \mu\varepsilon H_\varphi = 0. \tag{30}$$

Equation (30) is to be solved subject to the following conditions on the boundary

$$H_\varphi = 0, \qquad \text{for } r = 0$$

and

$$\hat{n} \cdot \nabla H_\varphi + \frac{n_r}{r} H_\varphi = 0 \tag{31}$$

where $\hat{n}$ is the unit vector normal to the surface of the boundary.

Having determined H_φ, the components of the electric field are obtained by the relations

$$E_r = \frac{j}{\omega\varepsilon}\frac{\partial H_\varphi}{\partial z}$$
$$E_z = -\frac{j}{\omega\varepsilon}\left(\frac{1}{r}\frac{\partial}{\partial r}(rH_\varphi)\right). \quad (32)$$

C. Numerical Solution of the Nonlinear Eigenvalue Problem

The breakdown equation to be solved numerically reads

$$D\left[\frac{\partial^2 n}{\partial z^2}+\frac{1}{r}\frac{\partial}{\partial r}\left(r\frac{\partial n}{\partial r}\right)\right]+(\nu_i(E)-\nu_a(E))n=0 \quad (33)$$

with $n(z, r) = 0$ on the metal boundaries of the resonator. The modeling of the physical quantities appearing in (33) is here made more carefully than in the previous analytical and semianalytical investigations. In particular, the diffusion coefficient and characteristic frequencies of the problem are taken as [9]

$$D \approx \frac{10^6}{p} \quad \mathrm{cm}^2/\mathrm{s}$$
$$\nu_i \approx p\cdot 5\cdot 10^{11}\exp[-73(E_e/p)^{-0.44}] \quad 1/\mathrm{s}$$
$$\nu_a \approx p\cdot 7.6\cdot 10^{-4}\left[\frac{E_e}{p}\left(\frac{E_e}{p}+218\right)\right]^2 \quad 1/\mathrm{s}. \quad (34)$$

In (34), the effective electric field E_e should be measured in volts per centimeter and the pressure p in torr. The true (rms) electric-field strength E_{rms} is related to the effective electric field through the pressure dependent relation

$$E_e^2 = \frac{E_{\mathrm{rms}}^2}{1+(\omega/\nu_c)^2} \quad (35)$$

where $\nu_c = p\cdot 5\cdot 10^9$ 1/s is the collision frequency between the free electrons and gas atoms. Equation (33) is not of the simple Sturm–Liouville form considered previously, and even a numerical solution is not straightforward. However, it has been found convenient to solve the equation in the following iterative manner. We write the equation in the form

$$D\nabla^2 n+\lambda\frac{\nu_{\mathrm{net}}\left(ys(z, r)\right)}{y}n=0 \quad (36)$$

where $s(z, r)$ denotes the normalized form function of the electric field in the cavity (cf. the function $s(x)$ in our previous analysis) and y is a guess of the actual eigenvalue λ.

If we set y equal to an arbitrary value in (36), the equation becomes an ordinary eigenvalue problem that is directly solvable for $\lambda = \lambda(y)$ using MATLAB's PDE Toolbox. The problem is to find the y for which the solution of (36) gives an eigenvalue equal to y. Since the formulas for the ionization and attachment frequencies are only valid for $5 \le E_e/p \le 60$ (V/cm · torr) and $E_e = y\cdot s(z, r)$, we infer that y should span the interval $5p \le y \le 60p$. This interval is then stepped in equidistant steps to find $\lambda = \lambda(y)$. The solution of the subsequent equation $\lambda(y) = y$ is the desired value of λ.

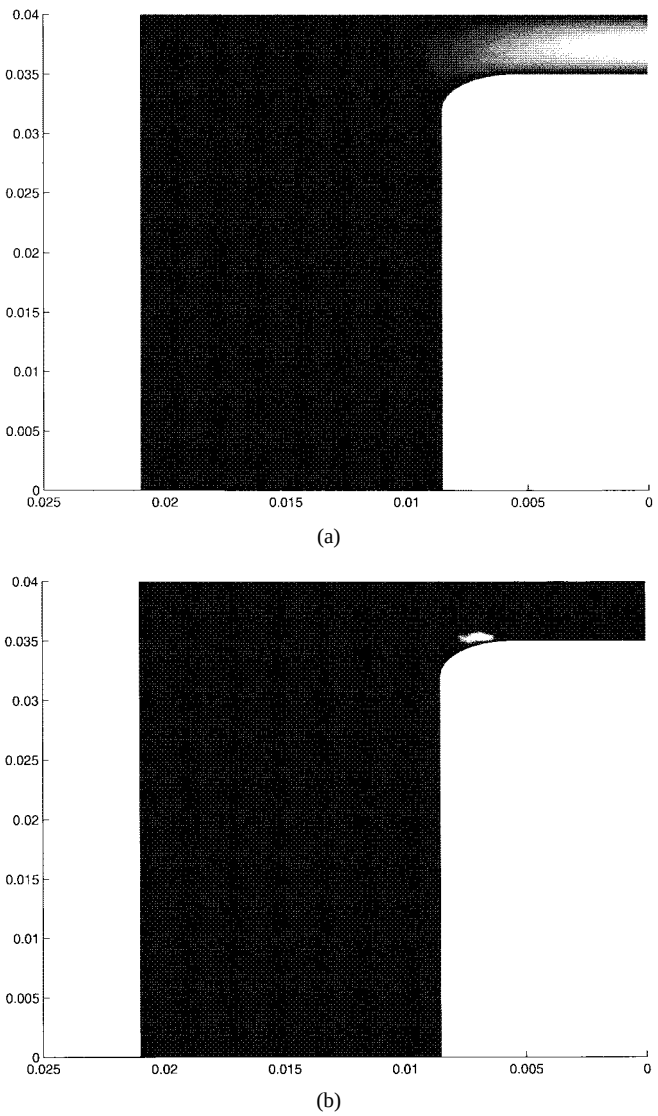

Fig. 2. Geometry of a rod resonator, as well as numerically obtained results for the electron density distribution at the breakdown threshold. Note the shift of the center of localization of the electron distribution as the pressure changes from: (a) 10 torr to (b) 760 torr.

D. Numerically Obtained Results

Some illustrative examples of the numerical simulation results are given in Fig. 2, which shows the electron density distribution at the breakdown threshold. The numerical computations have been made for a cylindrical rod resonator with the data: resonator frequency $= 1639$ MHz, cavity diameter $= 42.0$ mm, cavity height $= 40.0$ mm, rod diameter $= 17$ mm, rod height $= 35$ mm and rod-edge curvature radius $= 3.0$ mm. Several of the physical features discussed in the previous sections are clearly seen in the numerical results. In particular, we note that, at high pressures, the breakdown process is a very local phenomenon, which initiates in the region of highest local field enhancement at the top edge of the rod. This is typical for attachment-dominated breakdown. However, at lower pressures, the picture becomes quite different. Here, the diffusion loss becomes important, the resulting effective diffusion length becomes larger than the dimension of the region where the electric field is largest, and a large electron cloud spreads

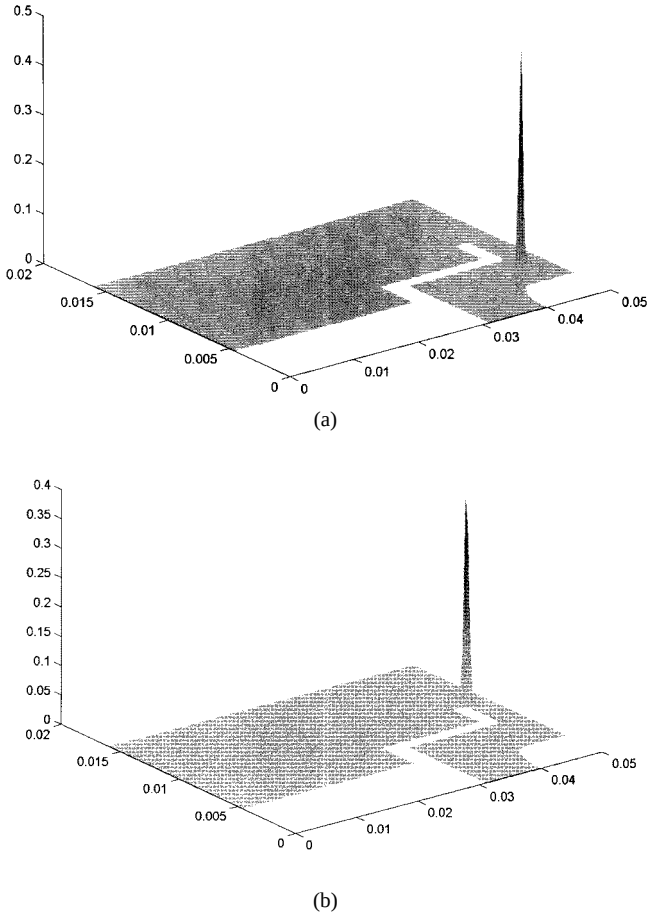

Fig. 3. Numerically obtained results for the electron density distribution at the breakdown threshold in a resonator with a more complicated geometry. Note the different localization of the two electron density eigenmodes shown in: (a) (mode 1) and (b) (mode 2).

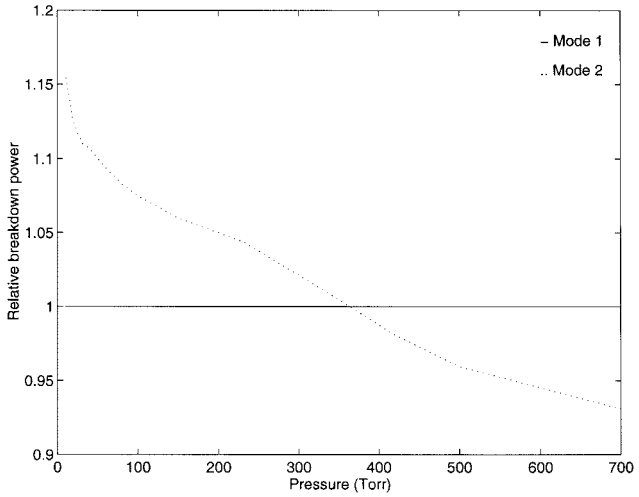

Fig. 4. Detailed picture of the crossing of the breakdown curves for the two modes shown in Fig. 3.

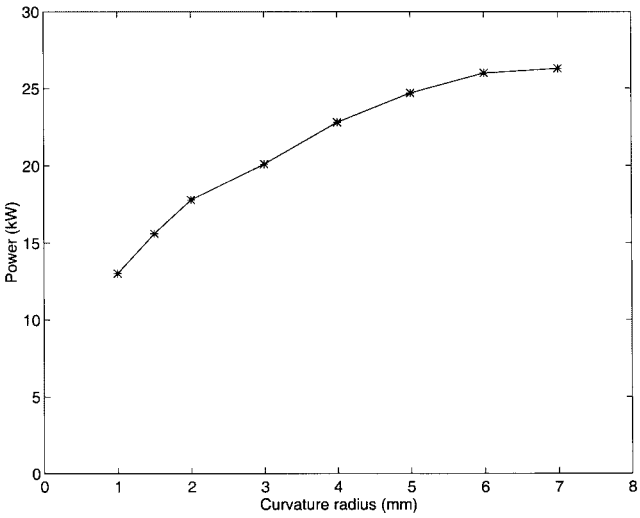

Fig. 5. Numerical results for the breakdown threshold power as a function of the curvature radius of the edge of the rod ($p = 760$ torr) in the resonator shown in Fig. 2.

out in the gap between the top of the rod and cavity wall. This picture is a direct verification of the physical conclusions about breakdown in diffusion/attachment-dominated situations in strongly inhomogeneous fields discussed in the previous section.

This change of localization of the electron density, which may occur in a complicated geometry, is further demonstrated in Fig. 3. In this case, a resonator tuning screw in the center, together with the resonator rod, provide a high field region in addition to the one at the edge of the hat, which will cause breakdown to be initiated in different regions at high and low pressure, respectively. In such situations, (36) provides at least two physically feasible solutions as the two modes with the lowest eigenvalues. At low pressure, the mode showing a predominance of electron density at the center have the lowest eigenvalue and, thus, sets the limit, whereas at high pressure, the mode having high electron density at the edge of the hat sets the limit. The crossover region is at approximately 400 torr. In Fig. 4, a corresponding "mode crossing chart" is shown.

A further aspect of the importance of local high electric field regions was also analyzed numerically. It is well known that sharp metal corners give rise to locally very high fields and that a careful design should avoid such features, e.g., by rounding off the corners. The effect on the threshold breakdown power of varying the curvature radius of the rod edge is shown in Fig. 5. It is clearly seen how the breakdown power decreases with decreasing curvature radius. In fact, the breakdown power for smoothly rounded corners is a factor of two larger than that for sharp corners.

VII. n Analytical–Experimental Approach for Breakdown Predictions

We will conclude the predictive analysis, by presenting a simple complementary approach for extrapolating low-pressure breakdown data for resonators and filters to higher pressures. The method relies on measurements of the actual breakdown threshold at low pressures, where the breakdown power is also low, which makes it possible to accurately extrapolate the breakdown threshold over a wide range of pressures up to atmospheric pressures. There, the

corresponding breakdown power levels are more than 20 dB higher than for the low-pressure bench marking measurements.

The physical basis of the approach is the analysis in Sections III–V, where the relative importance of diffusion and attachment in determining the electron density scale length are discussed. The determination of the density scale length can be done *a priori* using numerical means, as was demonstrated in Section VI-D, but it may also be determined empirically by experimentally determining the breakdown threshold at low pressures. Having determined the diffusion length L_D (or, equivalently, the density scale length at low pressures), which is a geometrically determined quantity, an extrapolation valid for the whole pressure range can usually be made, at least for not too complicated geometries.

In a straightforward version of this approach, we can take the breakdown threshold as given by (4), where the characteristic scale length L_{eff} is taken as the diffusion length that is unknown, but determined by the geometry of the configuration [cf. (27)]. Using a simplified [as compared to (34)] approximation for the net ionization frequency of air (e.g., [10], [11]), we have

$$\frac{\nu_{\text{net}}}{p} = 4 \cdot 10^7 \left[\frac{(E_e/p)}{100}\right]^{5.33} - 6.4 \cdot 10^4 - \frac{D}{pL_D^2} \tag{37}$$

where E_e is the effective electric field in volts per centimeter, p is given in torr, D in centimeters squared per second, and L in centimeters. This implies that the breakdown condition can be written

$$\begin{aligned} E_b &= E_b(f, p; L_D) \\ &= 3.75 \cdot p \left[1 + \left(\frac{2\pi f}{\nu_c}\right)^2\right]^{1/2} \left(\frac{D}{pL_D^2} + 6.4 \cdot 10^4\right)^{3/16} \end{aligned} \tag{38}$$

where E_b is the real rms electric field, and the factor 3/16 is a rational approximation of 1/5.33.

Expression (38) contains one unknown parameter, the characteristic length L_D, which determines the curvature of the Paschen curve [1] as a function of pressure in the low-pressure region. In order to relate data to expression (38), an additional unknown, the coefficient of proportionality between the square of the electric field and the input power of the resonator, is needed.

The analysis proceeds as follows. The mean breakdown power is determined for a sequence of input powers at the lower part of the Paschen curve. This set of points is then approximated by a number of Paschen curves [i.e., curves of the form given by (38)] with a fixed set off and variable scale lengths L_D. In order to choose an optimal L_D, a penalty function is constructed, essentially being the sum of the deviations from the mean predicted breakdown threshold at $p = 760$ torr for different L_D. The penalty function is used to find the optimal L_D, which is then inserted into (38) to give a prediction for the breakdown threshold of the resonator over a large range of pressures, including, in particular, the medium-to-high pressure region where actual breakdown tests are more difficult to perform due to the high power necessary to cause breakdown. An example of an application of this procedure will be given in Section VIII.

However, this approach must be used with some caution. In a complicated design involving strongly anisotropic diffusion geometry, the above concept of a unique (one-dimensional) scale length, which characterizes the diffusion over the whole pressure range, may be too simplified. In such geometries, the density scale length may, in fact, depend on pressure as the electron density distribution changes center of localization in the device. Examples of this were given in the previous section (cf. Fig. 2) and also in the form of the mode-crossing phenomenon (see Fig. 3). From a physical point-of-view, it seems reasonable that such mode relocalization or even mode crossings may occur since, e.g., at high pressure, the extension of the high-field region together with the attachment process, rather than the confining geometry, tend to limit the extension of the electron cloud.

VIII. Experimental Results and Comparison with Theory

A. Introduction

An important practical problem when comparing theory and experiments is to assess the actual electric field in the resonator from the power fed into it. However, although the electric field inside the resonator is not directly available, it can be inferred from the total stored energy W and the Q-value of the cavity according to

$$\begin{aligned} W &= \varepsilon \int\int\int E_{\text{rms}}^2 \, dV \\ P &= \frac{\omega W}{Q}. \end{aligned} \tag{39}$$

In (39), the dissipated power means the average power dissipated in all the connection ports in addition to the internal losses. Usually, a two-port is considered, and the power is fed into the input port from a generator. In (40), we give a slightly more useful and detailed version of the second relation of (39), valid for a resonator at resonance, having incident power P

$$\begin{aligned} P &= \frac{\omega_0 W}{Q_{\text{eff}}} \\ Q_{\text{eff}} &= \frac{4Q_L^2}{Q_{e1}} \end{aligned} \tag{40}$$

where Q_{e1} is the external Q for the input port and Q_L is the loaded Q for the entire resonator. Thus, using the numerically found mode structure in the resonator, the strength of the electric field in the resonator can be related to the measured power level by means of (39) and (40).

B. Comparison Between Theoretical Predictions and Experiments

In an experimental study, the breakdown strength of two rod resonators was determined as a function of gas pressure and the results were compared with the corresponding theoretical predictions. The measurements were done by fixing the input power level to the resonator to certain levels, and for each power level, lower the pressure until breakdown occurred, at which point power and pressure were recorded. The procedure

was repeated five times for each power level with change of air in the resonator to exhaust breakdown products between successive tests. Breakdown was detected by measuring the sudden decrease in transmitted power, which signals that the global wave propagation properties of the resonator changed.

In order to be able to investigate breakdown under well-defined conditions, a single resonator was constructed and tested for breakdown. A 73-mm-long rod made of Cu with diameter 9 mm was inserted into an Al cavity of 74-mm height and diameter 30 mm. Thus, in this case, the air-gap to the silver-coated lid is only about 1 mm. The edge of the rod has a 2.5-mm curvature radius in order to avoid a sharp edge. The resonator had two ports, each with an external Q of 134. The internal Q of the resonator was 2050.

A second experiment was done on a specific (classified) Allgon product, (no data on the geometries are given, but it is of a similarly simple shape as that of Fig. 2), for rather small pressures ($p < 100$ torr) where the breakdown threshold easily could be reached. In this case, there were four resonators arranged into an approximate Chebyshev filter of 15-MHz bandwidth. According to the algebra of an ideal lumped-element network showing this Chebyshev transfer function, the two inner resonators would experience the highest amount of stored energy at matched operating conditions [13].

The experimental results obtained for the specially designed single resonator are summarized in Fig. 6. The mean breakdown pressure was determined experimentally for resonator pressures ranging from 30 to 500 torr. The agreement with the fully numerical results is shown to be good over the considered pressure range. The numerical results are apparently predicting a somewhat lower value than what is observed from the average breakdown threshold. This difference can partly be explained as due to the fact that theory predicts the breakdown level assuming that there are always free electrons available to initiate the ionization process. Thus, if there are no free electrons, the resonator can withstand higher power. This implies that, in the experiment, where the pressure is decreased in time, the time delay for a first electron to appear tends to spread out the measured breakdown points in the direction of low pressure.

In the case of the semianalytical approach, the corresponding penalty function was found to have a pronounced minimum for a diffusion length of $L_D \approx 0.4$ mm, using the experimental points at low and intermediate pressures. The corresponding extrapolation curve is also included in Fig. 6. The curve has two free parameters, the geometrical length of diffusion $L_D = 0.4$ mm and an offset of -29.3 dB determined by the relationship between input power and the obtained electrical field in the structure. The agreement between the semianalytical and the fully numerical predictions, as shown in Fig. 6, is also very good for the extrapolated region up to atmospheric pressure.

The corresponding comparison for the commercially available Allgon product mentioned above is shown in Fig. 7 and, again, shows very good agreement. The considered pressure range implies that we are investigating breakdown processes, which are diffusion dominated for the lowest pressures to become diffusion/attachment dominated for the highest considered pressures. Breakdown tests at atmospheric pressures could not be done with the existing equipment, but a pulsed test has been made at $p = 760$ torr with microwave pulses of pulse length > 1 μs (which should be sufficient to cause breakdown if it should occur). The resonator sustained 12-kW peak equivalent power, which is consistent with the predictions. This survival point is shown in Fig. 7.

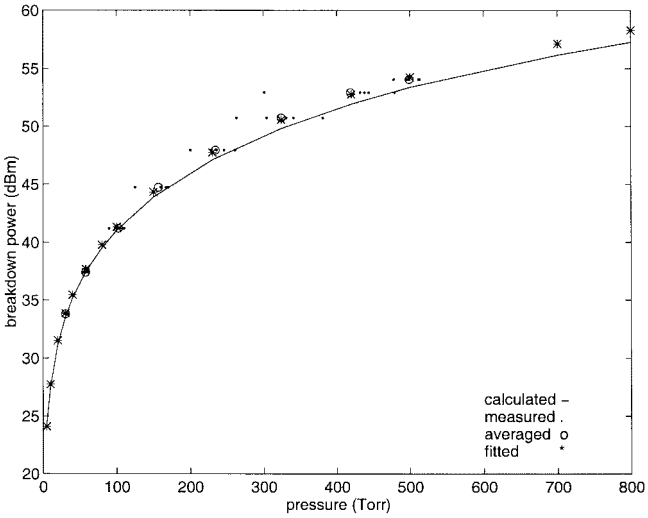

Fig. 6. Comparison between experimental results and theoretical predictions for the breakdown threshold as a function of gas pressure for the specially designed single resonator. Experimental points (·), the average of five experimental points for given input power (o), the numerically obtained curve (—) and the semianalytical extrapolated points (*).

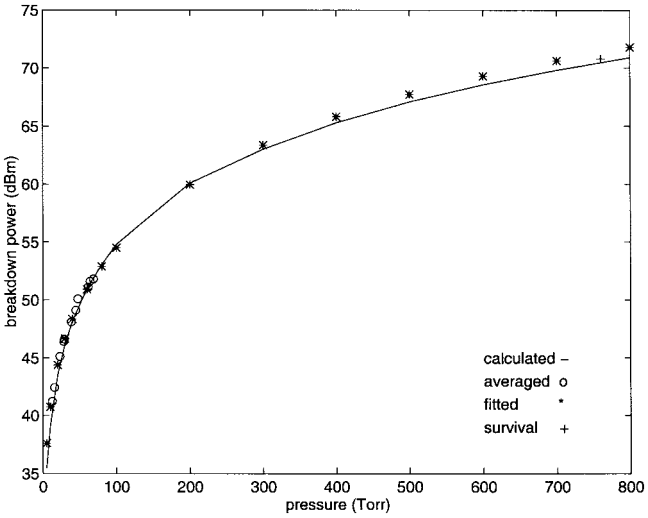

Fig. 7. Comparison between experimental results and theoretical predictions for the commercially available Allgon product. The result of the survival test is marked (+). Other notation as in Fig. 6.

IX. Conclusions

In this investigation, we have considered several aspects of microwave breakdown in resonators and cavities. The first part of the analysis has emphasized the main physical properties of microwave-induced breakdown in the presence of inhomogeneous electric fields—a feature which introduces important complications in an analysis of the processes and the dynamics involved in the breakdown process. It has been

demonstrated that, using an approximate approach based on direct variational methods, significant progress can be made in formulating explicit and simple breakdown criteria for physically and technically important situations.

In these first studies, comparatively explicit expressions for the microwave electric field have been assumed. Although this is a legitimate approach in simpler geometrical situations, many technically important situations involve more or less complicated geometries where an analytical determination of the mode structure of the microwave field as well as of the concomitant characteristic density scale length are impossible. In order to handle such situations, two complementary approaches have been developed.

The first approach is a semianalytical one, which relies on the fact that the diffusion losses are determined by a characteristic diffusion length being determined by the geometry of the resonator. Although this scale length can not be determined analytically for a complicated geometry, it can be inferred by numerical fitting procedures from experimental breakdown data in the low-pressure region where breakdown tests are easy to perform. Having determined the characteristic diffusion length, the unknown parameter in the breakdown threshold condition is known and the formula can be extrapolated to medium and high pressures with some confidence.

The second approach involves first solving Maxwell's equations in circular–symmetric geometry in order to determine the associated mode structure of the field. This result is then inserted into the eigenvalue equation for the electron density, which determines the breakdown condition. Finally, the critical breakdown field is determined by solving the eigenvalue equation numerically.

In order to test the theoretical predictions, a series of breakdown tests were made on two different resonator designs, including a commercially available one. The comparison between theory and experiments shows very good agreement and we think that the obtained results encourage the use of the presented methods for predicting breakdown in resonators as a complement to high-power pulse testing at atmospheric pressure. By lowering the air pressure in the resonator or the cavity, a microwave discharge can be generated even at moderate power. There is an advantage in knowing what the pressure limit for the construction is, i.e., that a discharge most likely will occur at a certain pulse power and pressure. It is even possible to run continuous wave excitation in single or multicarrier configuration, thereby simulating a realistic transmission format, and nevertheless obtain a discharge at sufficiently low pressure. Some uncertainty, in the case of the method that involves extrapolation to atmospheric pressure, will necessarily follow for designs involving complicated geometries. However, used with some caution, the method should be a simple and useful tool for predicting breakdown in resonators and cavities at medium and high pressures.

The more complete and fully numerical test program for breakdown that has also been developed consists of two numerical steps—one, which solves the microwave-mode structure in the resonator or cavity and another that determines the breakdown condition once the mode structure is known. The predictions have been tested against experiments at small to moderate pressures, where breakdown tests are easy to perform, and the agreement is found to be very good. Thus, this numerical approach can be used as an efficient and accurate predictive tool for microwave breakdown in the design of resonators and filters even up to atmospheric pressures.

REFERENCES

[1] A. D. MacDonald, *Microwave Breakdown in Gases.* New York: Wiley, 1966.

[2] A. V. Gurevich, N. D. Borisov, and G. M. Milikh, *Physics of Microwave Discharges.* New York: Gordon and Breach, 1997.

[3] M. Epstein, "High-frequency breakdown of nonuniform gases in spatially varying fields," *Phys. Fluids*, vol. 11, pp. 896–902, 1968.

[4] J. T. Mayhan and R. L. Fante, "A variational formulation specifying the breakdown criteria for plasmas subjected to spatially nonuniform electric fields," *J. Appl. Phys.*, vol. 40, pp. 449–453, 1969.

[5] ———, "Microwave breakdown over a semi-infinite interval," *J. Appl. Phys.*, vol. 40, pp. 5207–5211, 1969.

[6] C. D. Maldonado and I. L Ayala, "Diffusion-controlled breakdown in cylindrical microwave cavity excited in the TM_{0n0} mode," *J. Appl. Phys.*, vol. 43, pp. 2650-2656, 1972.

[7] M. A. Herlin and S. C. Brown, "Electrical breakdown of a gas between coaxial cylinders at microwave frequencies," *Phys. Rev.*, vol. 74, pp. 910–913, 1948.

[8] Jahnke, Emde, and Lösch, *Tables of Higher Functions.* Stuttgart, Germany: Teubner Verlagsgesellschaft, 1966.

[9] W. Woo and J. S. De Groot, "Microwave absorption and plasma heating due to microwave breakdown in the atmosphere," *Phys. Fluids*, vol. 27, pp. 475–487, 1984.

[10] W. C. Taylor, W. E. Scharfman, and T. Morita, *Advances in Microwaves Vol. 7*, L. Young, Ed. New York: Academic, 1971.

[11] D. Anderson, M. Lisak, and T. Lewin, "Generalized criteria for microwave breakdown in air-filled waveguides," *J. Appl. Phys.*, 1989, vol. 65, pp. 2935–2945.

[12] C. A. Balanis, *Advanced Engineering Electromagnetics.* New York: Wiley, 1989.

[13] G. L. Matthaei, L. Young, and E. M. T. Jones, *Microwave Filters, Impedance. Matching Networks, and Coupling Structures*. McGraw-Hill, 1964, ch. 15.

D. Anderson, photograph and biography not available at the time of publication.

U. Jordan, photograph and biography not available at the time of publication.

M. Lisak, photograph and biography not available at the time of publication.

T. Olsson (A'97), photograph and biography not available at the time of publication.

M. Åhlander, photograph and biography not available at the time of publication.